Geochimica et Cosmochimica Acta xxx (xxxx) xxx

Contents lists available at ScienceDirect

Geochimica et Cosmochimica Acta

journal homepage: www.elsevier.com/locate/gca

Photosymbiosis and nutrient utilization in giant clams revealed by nitrogen isotope sclerochronology

Daniel Killam [a,*], Shibajyoti Das [b], Rowan C. Martindale [c], Katelyn E. Gray [d], Adina Paytan [e], Christopher K. Junium [b]

[a] Biosphere 2, University of Arizona, 32540 S Biosphere Rd, Oracle, AZ 85623, USA
[b] Department of Earth and Environmental Sciences, Syracuse University, 204 Heroy Geology Laboratory, College of Arts and Sciences, Syracuse, NY 13244, USA
[c] Department of Geological Sciences, University of Texas at Austin, 2275 Speedway Stop C9000, Austin, TX 78712, USA
[d] Department of Plant and Soil Sciences, University of Delaware, 531 South College Avenue, Newark, DE 19716, USA
[e] Institute of Marine Sciences, University of California, Santa Cruz, 1156 High Street, Santa Cruz, CA 95064, USA

ARTICLE INFO

Associate editor: Hao-Jia Ren

Keywords:
Tridacna
Coral reefs
$\delta^{15}N$
Red Sea
Nano-EA-IRMS

ABSTRACT

Giant clams are reef-dwelling bivalves that reach unusual sizes through a partnership with photosymbiotic algae. To date, no shell-based biogeochemical proxy has been found which directly records the photosymbiotic development and health of these animals. We present new results showing a size-related decline in nitrogen isotopic values of shell-bound organic matter from the hinge layers of giant clams from the Northern Red Sea. In three of four tested shells, $\delta^{15}N$ values decline from >+4‰ at the juvenile stage to between 0 and −2.5‰ at maturity. These trends are consistent with a transition from heterotrophic nutrition early in the bivalve's life to receiving most of their nutrition from photosynthetic symbionts and external dissolved inorganic nitrogen at maturity. We find more muted declines or no change within the outer shell layer, with more inter-individual variability, which is likely related to the greater influence of the symbionts in the adjacent siphonal mantle of the animals. We use a von Bertalanffy-linked trophic model that uses $\delta^{15}N$ of nitrate and particulate organic matter to corroborate and explain the trophic transition in the ontogeny of the clams, and propose that high-resolution $\delta^{15}N$ measurements in bivalves could be used as a proxy for photosymbiosis and reef paleoenvironmental conditions in the fossil record.

1. Introduction

Many marine animals partner with photosynthetic algae to form mutualistic symbioses, with the symbionts providing sugars and other photosynthetic products to the host in exchange for nutrients and shelter (Lipps and Stanley, 2016). Photosymbiosis in mollusks is known to have evolved independently in multiple extant taxa, with obligate photosymbiotic relationships observed in giant clams (Tridacninae) and cockles in the subfamily Fraginae (Li et al., 2018). A variety of candidates for photosymbiosis have been identified among fossil bivalve taxa, including Cretaceous rudists (de Winter et al., 2020), members of the Jurassic *Lithiotis* fauna (Fraser et al., 2004; Posenato et al., 2013), Triassic alatoconchids (Yancey and Stanley, 1999), and others (Vermeij, 2013). Current evidence for photosymbiosis in bivalves is largely based on inference from diurnal (light-mediated) growth banding, morphology, and ecology/life habits while more direct geochemical proxies for photosymbiotic activity in fossil bivalves remain elusive. Diagenetic resetting and loss of primary shell material complicate attempts to identify unambiguous geochemical fingerprints of symbiosis applicable to the fossil record (Dreier et al., 2014).

Environmental and physiological signals can become intertwined in ways that make the isolation of either signal particularly difficult, as exemplified by prior attempts to find photosymbiotic signals in the carbon isotopic composition of shell carbonate (Jones and Jacobs, 1992; Killam et al., 2020). Such approaches could take the form of a known biogeochemical offset or daily oscillation in relation to light observed in modern photosynthetic bivalves, resulting from their internal physiology rather than external environment. Carbon isotopes (Jones et al., 1986) and daily oscillations in trace elements (de Winter et al., 2020) are confounded by external signals originating from the animals' reef environments (Jones and Jacobs, 1992; de Winter et al., 2022), rather than originating within the animals themselves and thus cannot be used as

* Corresponding author at: San Francisco Estuary Institute, 4911 Central Ave, Richmond, CA 94804, USA.
E-mail address: daniel.e.killam@gmail.com (D. Killam).

https://doi.org/10.1016/j.gca.2023.08.018
Received 14 June 2022; Accepted 21 August 2023
Available online 25 August 2023

proxies for photosymbiosis.

The nitrogen isotopic composition (denoted by $\delta^{15}N$ in per mil relative to air) of shell organic matter has proven to be a versatile record of bivalve diet and ecological dynamics. Such work has been used to trace anthropogenic eutrophication in watersheds and coastal environments due to fertilizer runoff or sewage (e.g., Carmichael et al., 2008; Graniero et al., 2016; Black et al., 2017; Darrow et al., 2017; Murray et al., 2019), as well as records of interannual fluctuations of source $\delta^{15}N$ in marine environments (e.g., Gillikin et al., 2017; Whitney et al., 2019; Das et al., 2021; Schöne and Huang, 2021; Peharda et al., 2022). The shell organic matter of giant clams and other bivalves is composed of intra- and inter-crystalline fractions containing polysaccharides, proteins, and lipids (Agbaje et al., 2017). The amino acids within the shell proteins represent the dominant source of nitrogen available for isotopic analysis. Prior workers have shown that bivalve shell $\delta^{15}N$ is correlated to the $\delta^{15}N$ of the animals' soft tissue (Carmichael et al., 2008; Graniero et al., 2016; Gillikin et al., 2017; Vokhshoori et al., 2022), allowing shell $\delta^{15}N$ to be used as an archive of the bivalve's nutrition postmortem.

$\delta^{15}N$ values of giant clam shell organic matter potentially record bivalve symbiosis. Giant clams harbor the same family of dinoflagellate photosymbionts as corals (Carlos et al., 1999) and possess low tissue $\delta^{15}N$ values in a similar range as corals and other mixotrophs (Kürten et al., 2014, Helber et al. 2021). Fossil photosymbiotic corals display a ~+7‰ depletion in $\delta^{15}N$ compared to coeval heterotrophic (filter-feeding) corals (Frankowiak et al., 2016; Tornabene et al., 2017). This large ^{15}N-depletion is posited to be a function of the lower relative trophic position of the photosymbiotic corals, intake of dissolved inorganic nitrogen (DIN) with lower $\delta^{15}N$ by the hosts, and internal recycling of host nitrogen waste by the symbionts. While prior studies have investigated the bulk shell $\delta^{15}N$ values of giant clams (Killam et al., 2021), no prior studies have investigated the variability of shell nitrogen isotopes in giant clams at the sclerochronological resolution necessary to observe changes over the lifespan of the animal.

Giant clams accelerate their symbiosis as they grow (Yau and Fan, 2012), with the symbionts increasing their uptake of host ammonium waste as the animal ages (Fitt et al., 1993). The host clam effectively drops in trophic level as it begins to feed on symbiont products more than external filter-fed nutrition (Klumpp et al., 1992). The host assists its symbionts by actively drawing in external DIN, primarily as nitrate and ammonium (Hawkins and Klumpp, 1995; Ip et al., 2020).

Changes in nitrogen sourcing are recorded in shell $\delta^{15}N$ of other calcifying organisms; for example, the seasonal variability of skeletal $\delta^{15}N$ in corals has received attention as a paleoenvironmental proxy in many regions of the world. It has been used to compare the historical and modern variability of monsoon-delivered aerosols (Ren et al., 2017) and acceleration of nitrogen fixation near the Great Barrier Reef due to anthropogenic eutrophication (Erler et al., 2020). To date, no high-resolution nitrogen isotope analyses have been conducted using giant clam shell carbonate, despite its demonstrated utility as an environmental indicator (Aharon, 1990). If giant clams directly record the isotopic variability of ingested DIN in their shell nitrogen isotopic values, this could represent a valuable high-resolution nutritional proxy applicable throughout the range of this species, from the Northern Red Sea to New Caledonia (Neo et al., 2017), as well as throughout their fossil record.

Previous analyses of giant clam shell organic matter have been limited by the very low organic matter content of giant clam shells (Dreier et al., 2014; Agbaje et al., 2017), which hindered isolation of the organic fraction by acid digestion methods. Recent advances in the analysis of the nitrogen isotopic composition of shell-bound organic matter now allow for the creation of a detailed record of reef bivalve symbiosis and nutrition (Gillikin et al., 2017; Whitney et al., 2019; Das et al., 2021; Peharda et al., 2022). Small samples of bivalve shell powder may be directly combusted and fed in a modified elemental analyzer coupled to a cryo-trapping/capillary focusing system paired to an isotope ratio mass spectrometer (nano-EA-IRMS). The nano-EA facilitates measurement of the organic nitrogen isotopic composition of 5–15 mg samples of powdered shell with as little as 0.01–0.05 weight % N (Polissar et al., 2009). With this improvement, the measurement of the evolution of nitrogen isotope ratios across the sequential shell diary of a giant clam (sclerochronology) is now achievable. Here, we investigate if a trophic decline in $\delta^{15}N$—indicative of this physiological transition from filter-feeding to photosymbiosis—can be detected through the life history of giant clams.

In this work, we describe analyses measuring the $\delta^{15}N$ values from sclerochronological samples representing the life history of multiple giant clam specimens collected in the Gulf of Aqaba, Northern Red Sea. These data allow us to create time series that record the nutrition and physiology of the animals during the development of their symbioses. We propose that the trends in $\delta^{15}N$ within the shells represent a record of photosymbiosis applicable to fossil shells, and we discuss practical and logistical considerations for selecting bivalve specimens in the fossil record that are candidates for photosymbiosis.

2. Materials and methods

2.1. Locality and sample collection/processing

In August 2016, four giant clam specimens were obtained from the Hebrew University of Jerusalem Museum. These shells had been collected illegally by poachers in Sinai, were confiscated by Israeli Border Security at the Egypt-Israel border crossing near Eilat, and subsequently donated to the museum (Fig. 1). We identified these shells as mature individuals of *Tridacna maxima* (shell H6, H2), and *Tridacna squamosina* (shell H5, H4) based on a taxonomic key used for identification of tridacnids in the Red Sea (Roa-Quiaoit, 2005). Additionally, we collected two juvenile shells of recently deceased *T. squamosina* (shells SQSA2 and 53) from the surf zone of the Interuniversity Institute in Eilat (29.501741°N, 34.917428°E), with permission from the Israel Nature & Parks Authority (permit number 2016/41334).

We sectioned the shells longitudinally along the axis of maximum growth for geochemical sampling (Fig. 2A). Sampling was conducted with a Dremel tool at 200 RPM using a Dremel 9906 tungsten carbide cutter, milling samples of carbonate powder along trenches parallel to the orientation of growth lines in the hinge and outer shell layers of the clams. Lines in the external growth layer follow the orientation of the bivalve's shell margin in life, while growth lines in the hinge and internal layer represent a record of the thickening of the shell (Gannon et al., 2017) (Fig. S3). The hinge and inner layer of the clams display annual growth lines, which result from the ~7–9 °C annual oscillations in sea surface temperature in the Gulf of Aqaba (Al-Rousan et al., 2003; Killam, 2018; Killam and Clapham, 2018; Killam et al., 2020, 2021). These lines were photographed with transmitted or reflected light and scaled for measurement with ImageJ software to produce an age model for the hinge growth layer of each individual; however, because we do not know the precise date of collection/death for the poached shells, the ages cannot be used as an absolutely dated chronology for the region.

2.2. Environmental data

From January 2003–2005, 59 sampling cruises were conducted embarking from the Interuniversity Institute in Eilat, Israel, proceeding along a series of stations following the shallow shelf of the Israeli and Jordanian coastlines of the Northernmost Gulf of Aqaba. A CTD-Rosette with 12-liter Teflon-coated GoFlo bottles was used to sample at varying depths from 0 to 20 m (the mixed layer). The water was sampled for dissolved nitrate $\delta^{15}N$ values, as well as particulate organic matter (POM) $\delta^{15}N$ values. Further description of the sampling methods and resulting isotopic analyses may be found in the Supplemental Materials.

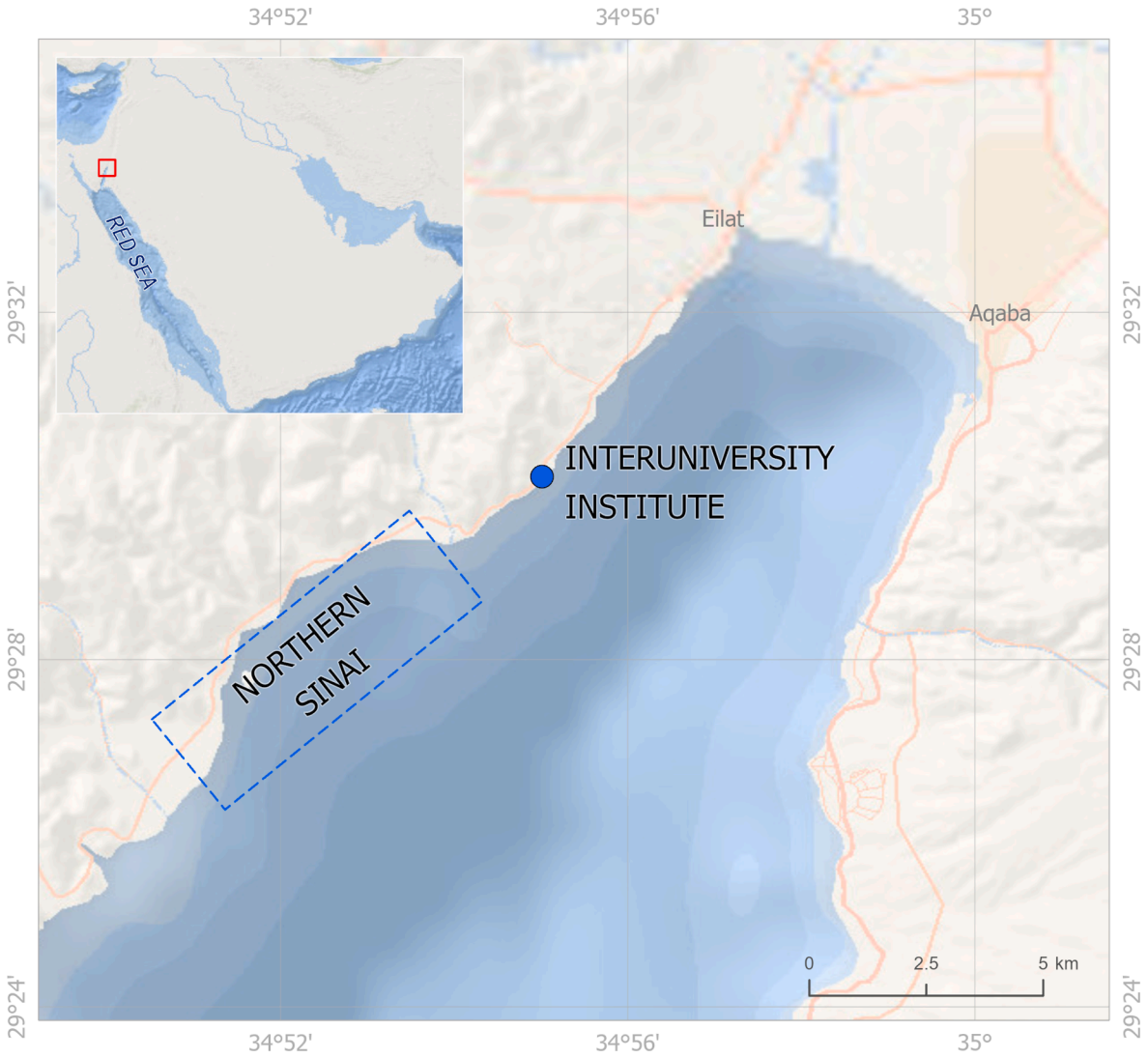

Fig. 1. Map of the study area, including the Interuniversity Institute in Israel (29.501741°N, 34.917428°E) and the suspected locational origin of the Sinai shells, as this region contains prominent resorts frequently visited by people crossing the border (located 29.491389°N, 34.9025°E).

2.3. Geochemical analysis

We sampled shell H2, H4, and H5 within the hinge and outer layers. H6 was only sampled in the hinge layer, as sponge borings in its outer layer left it unsuitable for geochemical analysis (Fig. 2A). For the two small juveniles collected in Israel, powder yield was too small to conduct high-resolution work, so we only extracted bulk samples averaging across the entire external shell layer. Samples of ~40 mg carbonate powder were collected in microcentrifuge tubes, homogenized, and partitioned into 5 mg, 10 mg, and 15 mg masses. These subsamples were loaded into tin capsules, evacuated and sparged with argon to remove interstitial atmospheric N_2, and subsequently combusted in an Elementar Isotope Cube EA coupled to an Isoprime Trace Gas analyzer. A similar analytical procedure regarding operation of the EA for the measurement of *Spisula solidissima* samples was outlined in Das et al. (2021). CO_2 and any CO resulting from combustion are trapped in a molecular sieve trap, while N_2 is captured by a silica-filled steel capillary trap cooled in a liquid nitrogen dewar. The N_2 is carried by a helium stream through an Agilent CarboBond column and into the Isotope Ratio Mass Spectrometer (IRMS) at the Geobiology, Astrobiology, Paleoclimatology, Paleoceanography Lab (GAPP Lab), Syracuse University.

We ran the subsamples in triplicate, correcting for the procedural blank using Keeling plots, with the intercept of the linear regression equation representing the $\delta^{15}N$ composition of the nitrogen emitted from the combusted shell material (see Supplemental Materials). The blank-corrected data are f normalized using a two-point correction scheme (Coplen et al., 2006) with the internal standard Peach Leaves ($\delta^{15}N = +1.98 \pm 0.4‰$), the IAEA-N2 ammonium sulfate standard ($\delta^{15}N = +20.4 \pm 0.3‰$), and the caffeine standards USGS 61 ($\delta^{15}N = -2.87 \pm 0.3‰$) and USGS 62 ($\delta^{15}N = +20.17 \pm 0.3‰$). All $\delta^{15}N$ values are expressed in per mil notation relative to atmospheric N_2. The error on the resulting final measurements is calculated as the standard error of the intercept on the Keeling plot (Fig. S1). Percent N values are calculated for each triplicate subsample by dividing the peak area by the total mass of the original sample and adjusting using standards with known mass percent. These triplicate results are then averaged to report an overall %N value for each sample. Data visualization and statistical analyses were conducted with R (R Core Team, 2013). All isotopic data are available in the Supplemental Materials.

2.4. von Bertalanffy growth modeling

We constructed a model of tridacnid somatic $\delta^{15}N$ in relation to shell/body growth and age based on prior isotopic measurements of Red Sea giant clams independent of our study's measurements. We applied a standard von Bertalanffy logistic growth equation previously used for

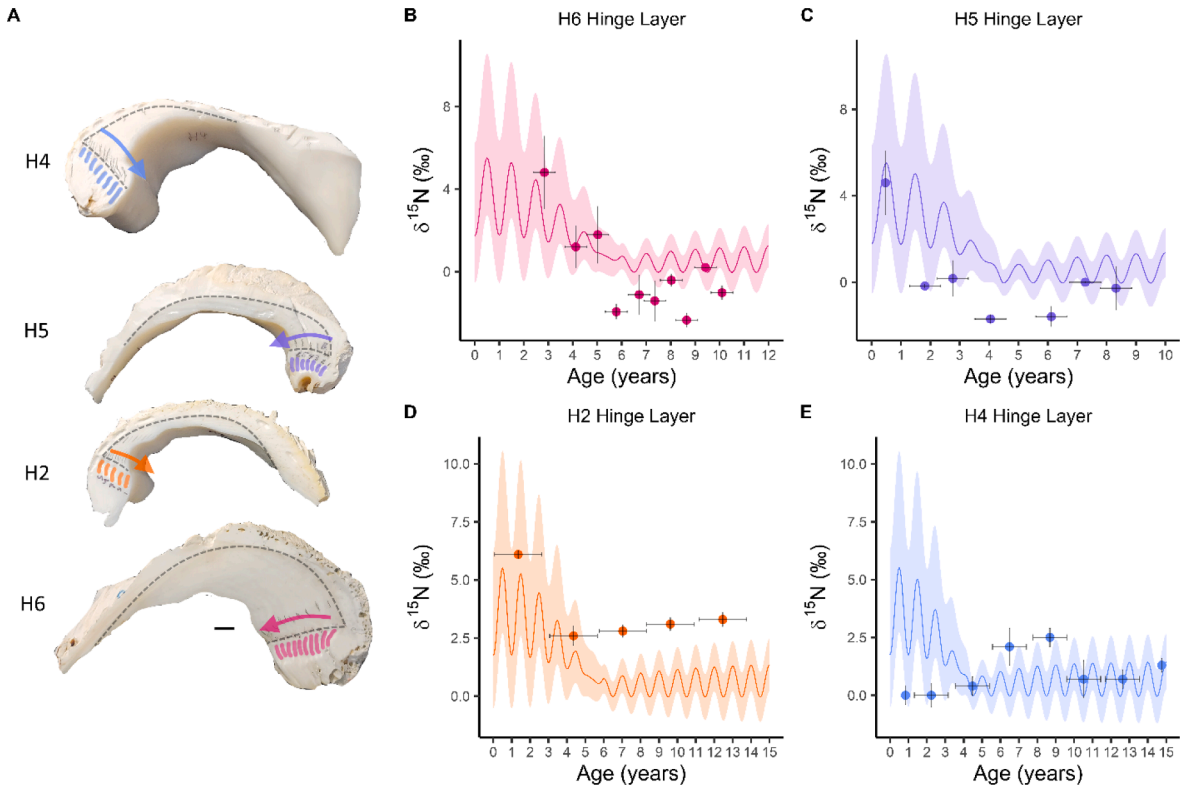

Fig. 2. A: Cross sections of shells H6, H5, H2, and H4, with the sampling tracks colored corresponding to the colors of the other plots in the diagram. Arrows represent the direction of the animal's growth. Curved black dashed lines highlight the position of the pallial line separating the hinge, outer and inner shell layers. Black bars represent 1 cm scale for each shell. B: Nitrogen isotope values for the hinge layer transect from shell H6 by age. Vertical error bars represent standard errors for $\delta^{15}N$ values and horizontal errors correspond to length of time in the age model averaged by each sampling track (also in C–E). Magenta band represents the $\delta^{15}N$ values produced by the physiological model described in this study for *T. maxima*. C: $\delta^{15}N$ values along the hinge layer for shell H5. Purple band represents the $\delta^{15}N$ values produced by the physiological model described in this study for *T. squamosina*. D: $\delta^{15}N$ values along the hinge layer transect for shell H2. Orange band represents the $\delta^{15}N$ values produced by the physiological model described in this study for *T. squamosina*. E: $\delta^{15}N$ values along the hinge layer for shell H4. Blue band represents the $\delta^{15}N$ values produced by the physiological model described in this study for *T. maxima*.

Tridacna (Munro, 1982) to model shell height as a function of time for *T. maxima* and *T. squamosina*.

$$h(t) = H_{\infty}(1 - e^{-kt}) \quad (1)$$

We then converted that shell height to tissue mass based on a standardized equation developed across multiple giant clam species (Hardy and Hardy, 1969). Growth constants (k), asymptotic heights (H_{∞}), height-weight conversions and season of recruitment for both species were obtained from prior literature on giant clams in the Red Sea and elsewhere (Hardy and Hardy, 1969; Roa-Quiaoit, 2005; Chan et al., 2008; Richter et al., 2008; Mohammed et al., 2019; Killam et al., 2021).

Giant clams grow more rapidly in summer, with growth increments being twice as wide when glams grow in warm waters (up to 31 °C) compared to lower winter temperatures (~22 °C) (Lucas et al., 1989). To simulate their response to temperature variation in the Gulf of Aqaba, which ranges from 21 to 28 °C, we varied the *k* growth constant according to a seasonally varying sinusoid following a seasonally varying von Bertalanffy approach previously applied to fishes (Pitcher and Macdonald, 1973), given by the equation::

$$k' = k + 0.005(cos(2\pi^{*}t) + 10) \quad (2)$$

We modeled the nonlinear accelerating intake of environmental DIN by giant clams as a quadratic polynomial relating animal shell height to grams of N ingested per year (Hawkins and Klumpp, 1995).

$$DIN\ \ demand = 0.0067595^{*}h^{2} \quad (3)$$

We modeled the $\delta^{15}N$ of the particulate organic matter (POM) of the surface layer of the Red Sea with the following sinusoidal equation:

$$\delta^{15}N_{POM} = 1.5^{*}cos(2\pi^{*}t) + 2.2 \quad (4)$$

The $\delta^{15}N$ of environmental nitrate was represented by a sinusoid approximating the seasonal oscillation in $\delta^{15}N_{nitrate}$ in the surface layer of the Red Sea, based on the values from the environmental sampling.

$$\delta^{15}N_{nitrate} = -1.9^{*}cos(2\pi^{*}t) + 1.1 \quad (5)$$

We also included a range of potential values in the model deviating positively and negatively from those sinusoids based on the within-season standard deviation in nitrate and POM $\delta^{15}N$ observed during the cruise sampling (described at greater length in Section 3). A cold season was defined as lasting from October-March, and a warm season from April-September.

Ammonium sourced from remineralization of N in sediment pore spaces and the reef framework has been observed to approximately equal the concentration of nitrate at the reef sediment–water interface in the Gulf of Aqaba (Rasheed et al., 2002). There are no known measurements of the $\delta^{15}N_{ammonium}$ in the Gulf of Aqaba, but as a first-order approximation, we set the $\delta^{15}N$ of the reef framework organic matter feeding into remineralization at +1.5‰, the mean isotopic value of photosymbiotic corals from the region (Alamaru et al., 2009; Kürten et al., 2014). Remineralization in oxygenated sediments fractionates nitrogen by up to −2.3‰ (Möbius, 2013). We applied that negative factor and then computed $\delta^{15}N_{DIN}$ as the simple average of $\delta^{15}N_{ammonium}$ and $\delta^{15}N_{nitrate}$ from the sampling cruises, assuming they had equal concentrations through the year.

The clam's somatic growth was calculated in 0.05-year increments (~18 days) from the derivative of the von Bertalanffy-sourced growth in

tissue mass. The nitrogen content of the clams' organic matter was calculated based on prior observations of ~70% protein by body weight in giant clams (Mahmoud et al., 2018) and 17% nitrogen content in bivalve protein (Gnaiger and Bitterlich, 1984; Hawkins and Klumpp, 1995). We assumed the $\delta^{15}N$ of the clam's heterotrophically sourced integrated nitrogen to be elevated by 2.5‰ over POM, based on previous measurements of trophic enrichment of $\delta^{15}N$ among herbivorous and planktivorous primary consumers in the Northern Red Sea (Kürten et al., 2014). Finally, we modeled the isotopic transition in the animal induced by the change to ingested external DIN at the expense of heterotrophically-sourced nitrogen with a mass balance approach, assuming an increasing fraction of the clam's somatic nitrogen was delivered by direct ingestion of external DIN.

$$\delta^{15}N_{tissue} = (N_{tissue} - N_{external}) \times (\delta^{15}N_{POM} + 2.5‰) + \frac{N_{external} \times \delta^{15}N_{DIN}}{N_{tissue} + N_{external}} \quad (6)$$

The output was plotted relative to age to compare to our directly measured shell organic $\delta^{15}N$ results. All relevant R code is provided in the Supplemental Materials.

3. Results

3.1. Isotopic measurements

Shell H2 and H6 (*Tridacna maxima*) lived for 9 years and 11 years, respectively, as measured from internal growth lines (Fig. S2). Shells H4 and H5 (*T. squamosina*) lived for 15 years and 7 years, respectively. Along the hinge layer transects, two shells (*T. squamosina* shell H5 and *T. maxima* shell H6) show $\delta^{15}N$ values over +4‰ for the innermost increments deposited earlier in life (Fig. 2B–E). Those shells display similar rates of decline into later increments/years, while H6 shows intermediate values between 0 and +3‰ at 4–5 years in age (~1 cm into the hinge layer). H2 and H6 show values falling within a stable range between 0‰ and −2.5‰ after around 5 years in age. Shell H2 shows a similar transition, but with more positively offset values, starting at over +6‰ as a juvenile and transitioning to values between +2 and +3.5‰. Shell H4 differs from the others, showing a slight increase through life from 0 to ~+2‰.

In the outer shell layer for *T. squamosina* shell H5, the $\delta^{15}N$ signature through ontogeny is not as distinguishable as in the hinge layer, but values are above +0.5‰ from earlier sampling increments and between 0‰ and −1‰ for the last sampling increments (Fig. 3). Shell H4 shows a decline, from above +4‰ to nearly −1‰ at around 20 cm length, while shell H2 shows relatively static values around +2 to +3‰. Whole-shell outer layer values for the two Israeli juvenile *T. squamosina* vary; the bulk value from shell SQSA2, a 2 cm long individual, is comparatively enriched, at +7.7‰, while shell 53, a 2.5 cm long individual, is lower at +1.1‰ (Fig. 4).

The environmental $\delta^{15}N_{nitrate}$ values are higher in the cold season (mean +3.7‰, SD 2.4‰) than the warm season (mean +0.7‰, SD 2.4‰) (Fig. 5). Dust nitrate extract $\delta^{15}N$ values (Wankel et al. 2010) are depleted in ^{15}N in both winter and summer (cold: mean −2.1‰, SD 2.3‰; warm: mean −1.0‰, SD 2.1‰). $\delta^{15}N_{POM}$ values are inversely related to the nitrate observations, with higher values in the warm season (mean +3.0‰, SD 2.1‰) than the cold season (mean −0.7‰, SD 1.6‰).

Weight percent N content in the shells was low overall, with a broad range between 0.006% and 0.2% (mean 0.021%, SD 0.037%). The shell SQSA2, which measured 0.2%, was an outlier, with the next-most N-rich shell measuring 0.03%. There was no significant correlation between % N and distance along transects (Kendall correlation: $\tau = 0.015$, $p = 0.88$), with some transects showing positive trends and some negative

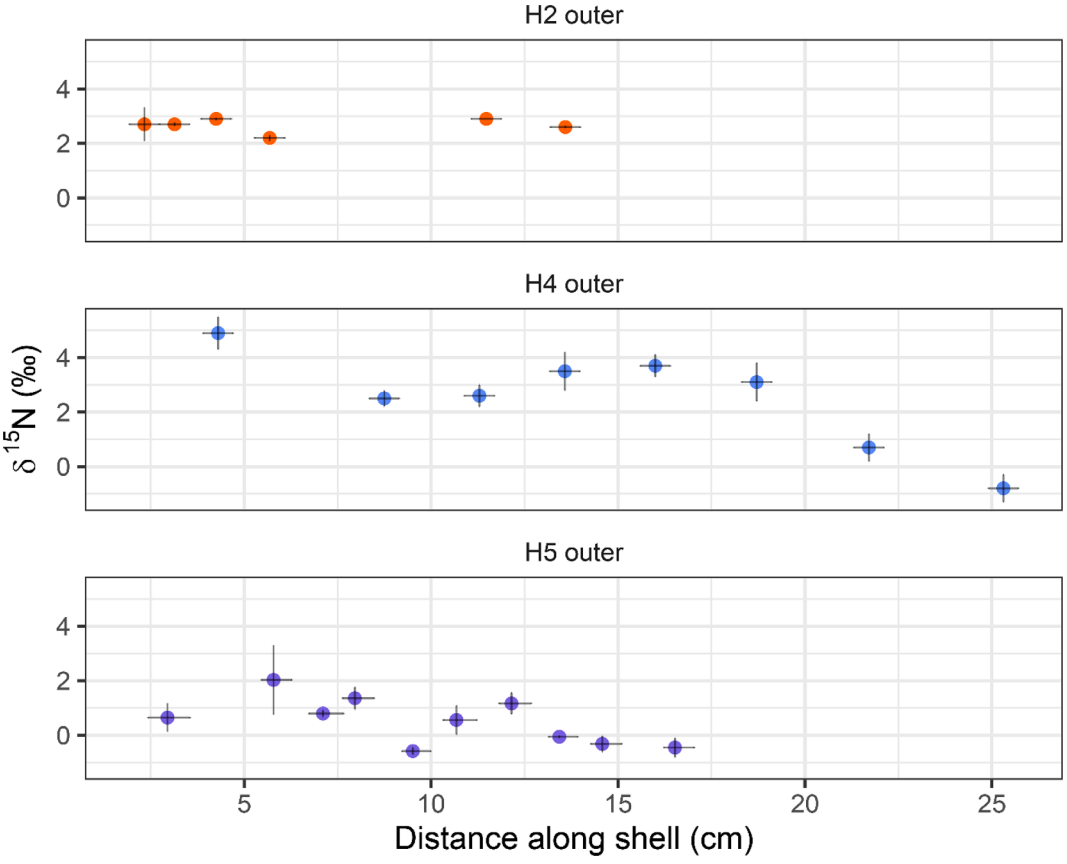

Fig. 3. Transects of $\delta^{15}N$ for outer layers of shells H2, H4, and H5 relative to distance along transect (equivalent to shell height). An age model was not applied to these values due to the lack of clearly visible growth lines in the outer shell layer.

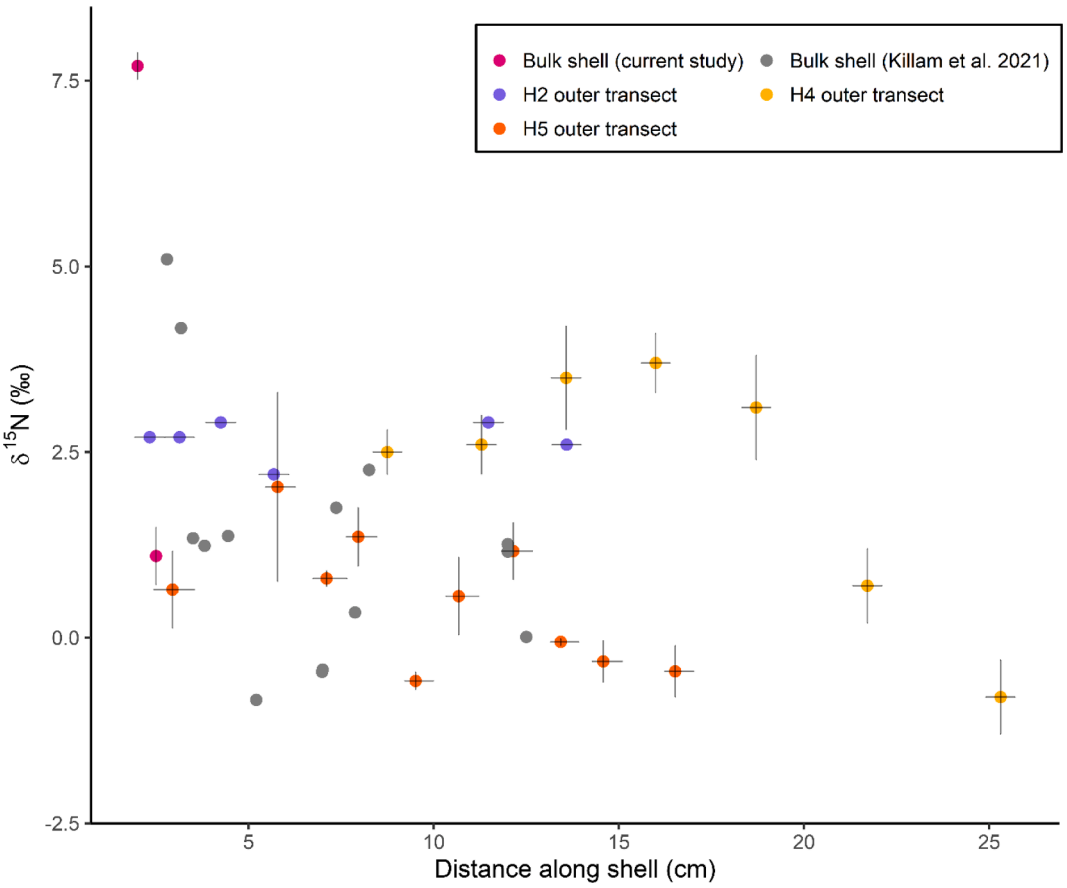

Fig. 4. Data from this study superimposed on whole-shell values (gray circles) from Killam et al. (2021), showing a decline in measured $\delta^{15}N$ with length. The body length of the whole-shell values is compared to the length along the individually sampled shell from the present study.

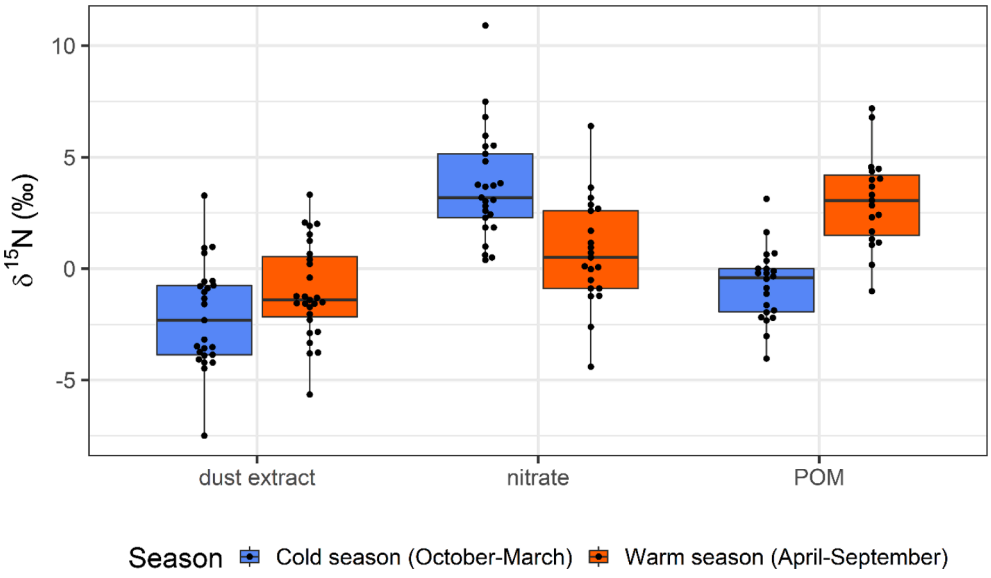

Fig. 5. Environmental $\delta^{15}N$ values of dust extract, nitrate and Particulate Organic Matter (POM), delineated by season of collection.

(Fig. S4). There was a significant positive correlation between %N and measured $\delta^{15}N$ (Kendall correlation: $\tau = 0.19$, $p = 0.04$), but the trend was not consistent between transects (Fig. S4).

When the outer layer data from this study are plotted in combination with the results from a prior experiment investigating whole-shell outer layer values from Red Sea clams, there is a negative relationship between the distance along shell and $\delta^{15}N$ among and within shells (Fig. 4) (Killam et al., 2021). There is divergence between individuals, with some displaying values as high as +7‰ early in ontogeny with later declines, and others such as H5, which display lower $\delta^{15}N$ values throughout their lives.

3.2. Model output

Modeled $\delta^{15}N$ values for both *T. maxima* and *T. squamosina* show ontogenetic declines from initial values between 0 and +9‰ representing fully herbivorous secondary consumers feeding on a highly heterogeneous $\delta^{15}N_{POM}$ pool, to values fluctuating between 0 and +4‰ after 5–6 years in age, the point at which the animal's heterotrophic nitrogen is overshadowed by ingested DIN (Fig. S2). The seasonal range in $\delta^{15}N$ is greater in earlier years of the record due to the larger seasonal disparity in $\delta^{15}N_{POM}$; when combined with the warm bias in tridacnid growth, this seasonal disparity leads to amplification of the summer positive values. Shells H6 and H5 show lower measured values than the modeled range later in life (Fig. 2B, C). Juvenile values of shell H4 are at the low end of the modeled range (Fig. 2E).

4. Discussion

4.1. Hinge layer transects as a record of photosymbiotic nutrition and external N supply

Sclerochronological transects of the hinge shell layer record ontogenetic declines in $\delta^{15}N$ values from +4‰ to 6‰ to near 0‰. These trends exceed the ontogenetic linked decline in $\delta^{15}N$ observed in non-symbiotic bivalves such as *Arctica islandica* (Schöne and Huang, 2021). Based on the strong relationship between tissue and bivalve shell $\delta^{15}N$ composition (Carmichael et al., 2008; Gillikin et al., 2017; Whitney et al., 2019), we propose that this ontogenetic decline indicates an increase in the influence of photosymbiosis on the inner mantle of the giant clams, the organ responsible for precipitating the inner and hinge shell layers (Gannon et al., 2017). The inner mantle of giant clams is symbiont-poor, unlike the outer mantle, but it still conducts active transfer of nitrogen-bearing compounds from the extrapallial fluid to the symbionts (Ip et al., 2017). Because filter feeding represents a larger share of the giant clam's nutrition and nitrogen supply earlier in life (Hawkins and Klumpp, 1995), its measured trophic position would be higher. As the clam grows and the nitrogen demand for its symbionts accelerates, it increasingly draws on externally-sourced DIN to supplement the nutrition of its symbionts (Fitt et al., 1993), lowering their trophic position from consumers down to that of primary producers and photosymbiotic soft corals from the region (Kürten et al. 2014). The DIN demand model was based on cultured *Tridacna gigas* specimens on Orpheus Island in the Great Barrier Reef. *T. gigas* and *T. maxima* are both heavily dependent on photosymbiosis for their nutrition (Elfwing et al., 2003; Yau and Fan, 2012) and may therefore display similar trends in external nitrogen demand relative to size. Our independent model suggests that externally sourced DIN represents the majority of the clam's nitrogen budget by around 5 years of age (Fig. S2).

This ~5-year age threshold could be significant to giant clam reproductive physiology; giant clams begin as males (protandry), and once they reach full female reproductive maturity at 3–4 years of age they produce both sperm and eggs (Lucas, 1994). There is variability in the timing of this transition, with individuals taking as long as five years (Chambers, 2007; Lachapelle, 2020), or even eight years (Lucas, 1994), depending on species and locality. Thus, the known life history of the animals could align with the size-linked photosynthetic progression of their symbiosis, and the fifth year might coincide with the first spawning event at which the Red Sea giant clams' energetic intake is sufficient to produce eggs for reproduction. More investigation into the link between photosynthesis, diet, reproductive development and sclerochemistry in giant clams is needed in order to determine whether variability in life history contributes to differences in timing of reproductive maturity.

Giant clams and their symbionts can acquire N from many sources, including recycled ammonia waste (Hawkins and Klumpp, 1995). The rate of internal N retention is high at nearly 95% (Hawkins and Klumpp, 1995), as very little N is later lost to excretion. This internal cycling does not adequately explain the depletion in $\delta^{15}N$ values as the animals develop. Instead, we propose that the negative trend is a result of increasing direct utilization of DIN available from the ambient waters of the Gulf of Aqaba.

The direct measurements of $\delta^{15}N_{POM}$ and $\delta^{15}N_{nitrate}$ represent the heterotrophic and autotrophic portion of the clams' nutrition, respectively. The POM values represent primarily phytoplankton, but also detritus and other suspended material that juvenile *Tridacna* ingest as filter-feeding generalists (Klumpp et al., 1992). The POM values for the Gulf of Aqaba show great seasonal variability, with higher values in summer than in winter. This disparity is likely due to the influence of diazotrophs like *Trichodesmium*, which display greater N fixation in the cooler months of the year, such as March (Foster et al., 2009). During blooms, $\delta^{15}N$ of POM will be depressed by the influx of ^{15}N-depleted diazotrophic-N (McClelland et al., 2003). By contrast, the $\delta^{15}N_{nitrate}$ values of the Gulf of Aqaba during January-March are comparatively ^{15}N-enriched due to the preferential assimilation of ^{14}N into POM by fixers and other phytoplankton, which often bloom in the winter and spring months (Berman and Gildor, 2022). In the summer, $\delta^{15}N_{nitrate}$ values are depressed by periodic dust storms common in the Northern Red Sea which carry ^{15}N-depleted compounds. The aeolian source of N can account for as much as 35% of the available nitrate in the summer months (Chen et al., 2007), particularly in the shallow habitat of *Tridacna*. This atmospherically-contributed nitrate pool has $\delta^{15}N$ values that are consistently lower than 0‰ due to photochemical fractionations in the atmosphere, with winter and summer $\delta^{15}N$ averaging −3.7‰ and −2.1‰, respectively (Wankel et al., 2010). This dust-borne nitrate represents a readily available source of supplemental nutrition for the clams during the summer months when giant clams' growth is fastest (Schwartzmann et al., 2011). The low $\delta^{15}N$ values that we observe later in ontogeny are consistent with atmospherically-sourced nitrate being a significant fraction of the N assimilated by *Tridacna*, effectively lowering the inferred trophic level from secondary consumer to near the N baseline.

Shell H4 does not show the same ontogenetic trend in its hinge layer as the other three individuals. Its $\delta^{15}N$ increased and then decreased through life, suggesting there is inter-individual variability in diet among clams from the Gulf of Aqaba. Nevertheless, the measured $\delta^{15}N$ of H4 still falls at the low end of the modeled range. The wide range of modeled shell $\delta^{15}N$ at the juvenile stage are a function of the observed range of $\delta^{15}N_{POM}$ which juvenile clams rely upon as their primary N-source. Clam H4 may have fed on more ^{15}N-depleted particulate matter as a juvenile compared to the other three specimens. Additionally, if clam H4 was able to grow in the winter months to a greater extent than the other measured clams, the proportion of the ^{15}N-depleted winter POM in its diet would be magnified compared to the other studied individuals. Bulk $\delta 1^{8}O$ measurements of clam H4′s outer layer reported in Killam et al. (2020) show some of the lowest values among the 48 studied *Tridacna* shells in that study, which correspond to a mean growth temperature of 25.2 °C, higher than the values from H2 (22.9 °C) or H5 (23.8 °C) (clam H6 was not measured). A warmer bulk-recorded $\delta^{18}O$ record would be consistent with clam H4 experiencing warmer winters and more continuous growth during those months when $\delta^{15}N_{POM}$ is lower.

The trend from higher to lower $\delta^{15}N$ values is present in shell H2, but isotopic measurements from later growth increments are higher than the modeled range. In contrast, when the isotopically depleted values assumed for $\delta^{15}N_{ammonium}$ are not included in the DIN term of the model (Fig. S5), the measured values fall within the modeled range. If clam H2 grew in a shallow lagoon site or other microenvironment with less exposure to remineralized ammonium from the reef framework, ingested DIN would be more ^{15}N-enriched than the other clams. Alternatively, the ammonium could have a more ^{15}N-enriched isotopic composition than assumed by the model, as many processes can act to enrich the $\delta^{15}N$ composition of sediment, such as partial assimilation (e.g., Lehmann et al., 2002). Future research is needed to measure the $\delta^{15}N$ of ammonium and its spatial variability in the Gulf of Aqaba to resolve

these questions.

The ontogenetic decline of $\delta^{15}N$ for the *T. maxima* shell H6 and *T. squamosina* shell H5 mostly follow the modeled output, aside from two values for each shell later in life, which fall below the expected range (Fig. 2B, C). This could be a function of the considerable variability in DIN available to the clams year to year. While we used idealized sinusoids approximating the isotopic composition of available POM and DIN, the interannual variability of this record could be much greater, depending on intermittent dust storms that vary greatly in their source air mass, dust intensity, and time of occurrence (Chen et al., 2007; Wankel et al., 2010). Atmospheric concentrations of water-soluble nitrate can vary between 20 and 100 nmol/m^3 in the Gulf of Aqaba (Chen et al., 2007). Additionally, other sources of DIN in the Gulf of Aqaba are still unmeasured in terms of nitrogen isotope mass balance, including interannual variation in N fixation rates (Foster et al. 2009), submarine groundwater discharge (Shellenbarger et al., 2006), bacterial denitrification within the clams' gills and other organs (though this likely imparts a relatively small influence on N) (Rossbach et al., 2019), and variability in seasonal upwelling (Labiosa et al., 2003; Badran et al., 2005).

The nitrate aerosols delivered by the dust storms largely originate from combustion-sourced NO_x gases and represent an anthropogenic signal in the clams' nutrition. Other pollution sources could also be recorded in the clam's $\delta^{15}N$ values, including human sewage, fertilizer, and aquaculture effluent. The Israeli portion of the Gulf of Aqaba hosted fish farms until the early 2000s, which harmed the health of reefs in that region (Loya, 2004). Clam shells from Israel from that period may record fish effluent-sourced ammonia, which is generally ^{15}N-enriched, as fresh fish feces measures +7‰ (Lojen et al., 2005). The Sinai clams of our study likely lived too far away from the Israeli coastline to integrate nitrogen sourced from Israeli aquaculture into their shells. Baseline $\delta^{15}N$ varies along a latitudinal gradient in the Red Sea (Kürten et al., 2014), and reefs in other regions also show great spatial variability in $\delta^{15}N$ values (Heikoop et al., 2000). Further work to measure $\delta^{15}N$ in giant clam shells from other regions or time periods must account for differences in the nitrogen pool available to the animals as well as ontogenetic changes.

4.2. Outer Shell Layer $\delta^{15}N$: Offset from the hinge layer and comparison to prior tissue measurements

The isotopic trends through the life of the clams studied were not consistent between the outer layers and the hinge layers. The transect across the outer layer of shell H5 displays more variability in $\delta^{15}N$ than its hinge layer. $\delta^{15}N$ decreases moderately from between‰0.5 and‰2‰ earlier in life to −0.5 to 1.1‰ later in its life. This is a less dramatic decline than in the hinge layer of that shell, where values decline from early values of ~4–5‰ to between 0‰ and −2.5‰ later in life. For shell H2, the variability is more limited, ranging between +2.2 and +−2.9‰ throughout the ontogenetic record. Shell H4 shows an opposing trend in the outer layer compared to the hinge layer, with a strong decline recorded through ontogeny from nearly +5‰ to below 0‰. These differences between the hinge and outer shell layers may be a function of the separate processes of calcification between the layers. The outer shell layer is calcified directly by the symbiont-rich, sun-facing outer siphonal mantle (Gannon et al., 2017), whereas the inner mantle is unpigmented and largely unexposed to light (Ip et al., 2017). The outer mantle harbors higher concentrations of proteins involved in the integration of DIN than the inner mantle (Teh et al., 2021) and may result in lower outer shell layer $\delta^{15}N$ earlier in the clam's life than is observed for the hinge shell layer.

The difference between the shell layers could also be a function of the differing microfabrics between the hinge and outer layers. While both are entirely aragonitic, the inner layer is prismatic (Pätzold et al., 1991), while the outer layer has been described as dendritic (Gannon et al., 2017) or crossed-lamellar (Agbaje et al., 2019) in microstructure. The shell layers may have different proteomic compositions integrating different amino acid fractions, but no prior study has compared the amino acid breakdown between layers within the same giant clam shell. Future study of compound-specific $\delta^{15}N$ values in *Tridacna* shells could shed light on a range of ecological and nitrogen cycle processes.

We suspect that the outer layer $\delta^{15}N$ is representative of the true $\delta^{15}N$ displayed by the animal's siphonal mantle at maturity. Prior measurements of tissue $\delta^{15}N$ of *T. squamosa* in the Northern Red Sea found a mean of +1.3‰ across 22 individuals, with a standard deviation of 1.2‰ (Kürten et al., 2014). The mean (1.7‰) and SD (1.5‰) of outer layer shell values in this study fall close to those values, supporting that the shell organic matter in the outer layer is isotopically homogeneous with the siphonal mantle responsible for precipitating that portion of the shell.

The whole-shell outer layer value of the small 2.5 cm *T. squamosina* shell 53 from Israel also falls within the expected range at +1.1‰, but shell SQSA2, a 2 cm long individual, shows a high value at >+7‰, suggesting that isotopic variability between individuals from the same locality may be present. When plotted in relation to outer shell bulk $\delta^{15}N$ values of Red Sea giant clams from a prior study (Killam et al., 2021), we observe that the $\delta^{15}N$ of some shells decline with distance along the shell, similar to the hinge shell layer (Fig. 4). Others have low $\delta^{15}N$ values throughout life, suggesting divergent ontogenetic pathways between individuals, leading to differing records between outer shell layers. Like other bivalves, giant clams' food sources are flexible, as they can ingest phytoplankton, zooplankton, or organic matter depending on availability (Lucas, 1994). The different juvenile clams could be recording diverse food sources in separate years of the Gulf of Aqaba, or differing rates of symbiotic development within the siphonal mantle. Differing food sources cause some individuals, such as shell H5, to have low $\delta^{15}N$ early in life while others, such as SQSA2, to have values as high as +7‰. High degrees of isotopic variability within and between individuals have previously been observed in nonsymbiotic bivalves as well (Whitney et al., 2019; Das et al., 2021; Peharda et al., 2022). Future work measuring giant clam shell $\delta^{15}N$ should incorporate individuals of various sizes, and ages, to allow for better resolution of individual differences. Testing more individuals could help delineate spatial or temporal gradients across the isoscape of giant clams from a region, analogous to those observed in corals (Fujii et al., 2020). While giant clams are a sensitive taxon and inherently sparse in their distribution, there is utility in maximizing sampling to potentially reconstruct gradients in their comparative utilization of autotrophy and heterotrophy across an environment.

The outer shell layer can be affected by biological interactions, compromising its utility for high-resolution nitrogen isotope work. The outer layer faces the external environment during the life of the animal, leading to colonization by boring epibionts while the clam is alive (Vicentuan-Cabaitan et al., 2014) and postmortem (Wisshak and Neumann, 2018). Contamination within and around the borings could reset the nitrogen isotope signal from the giant clam itself. In this study, we were unable to conduct a transect through the outer layer of shell H6 due to the extensive sponge borings (Fig. 2A) and in shell H5, erosion in the oldest (hinge-adjacent) portion of the outer layer prevented sampling from that area. Caution must be exercised in the selection of *Tridacna* shell specimens for $\delta^{15}N$ measurements due to the potential for bioerosion, particularly in the outer shell layer.

4.3. Percent nitrogen comparison to prior studies and relation to measured $\delta^{15}N$

Prior studies found high variability in organic content in the carbonate shell among giant clam species and individuals, with measurements of 0.05% to 0.17% for *Tridacna maxima* (Taylor and Layman, 1972; Dreier et al., 2014), 0.9% for *T. derasa* (Agbaje et al., 2017), and 1.83 wt% organic material for *T. gigas* (Agbaje et al., 2019). Organic material in bivalve shells is a mixture of protein, lipids, and other

compounds, with N forming a minority of the measured mass. Excluding the juvenile SQSA2, which was an outlier with 0.2 wt% N, our measured range between 0.004 and 0.035 wt% N is greater than the range in nitrogen content measured for *Spisula solidissima* (0.01–0.05 wt% %) (Das et al., 2021), *Pecten maximus* (0.07%) (Gillikin et al., 2017), and *Crassostrea virginica* (0.05–0.1%) (Black et al., 2017). A recent study reported weight % N ranging from 0.02% in the aragonitic, crossed-lamellar *Glycymeris pilosa* to 0.469% in the calcitic *Pinna nobilis* (Peharda et al., 2022). Generally, crossed-lamellar aragonitic bivalves show lower weight % N content.

While the low organic content presents a challenge for measurement of shell organic nitrogen isotopic values, giant clams may be studied sclerochronologically at higher resolution than other bivalves due to the nature of their massive shells and rapid growth. There was no significant relationship between distance along the shell and % N (Fig. S4A). Among the analyzed shells, we observed a weak relationship between % N and measured $\delta^{15}N$ which was not consistent between transects, corroborating a prior study of bulk shell organic material (Fig. S4B) (Killam et al., 2021). This contradicted the hypothesis that protein content in the shell would increase proportionally as the bivalves slowed in growth, creating more frequent yet slower growth lines later in life which are often higher in organic content (Schöne and Surge, 2012). The absence of correlation between age and nitrogen content, as well as between nitrogen content and measured $\delta^{15}N$, indicates that differential deposition rates of shell organic matter cannot explain dynamics in $\delta^{15}N$ within and between tridacnid shells.

4.4. Implications for the identification of photosymbiosis and paleoenvironment in fossil bivalves

A growing collection of bivalves in the fossil record have been proposed as potential hosts of photosymbionts based on morphological and ecological characteristics (Yancey and Stanley, 1999; Fraser et al., 2004; Posenato et al., 2013; Vermeij, 2013; Lipps and Stanley, 2016). These putative identifications have often called upon modern photosymbiotic bivalves such as giant clams and fraginids as models for potentially convergent traits. The identification of geochemical signals in giant clam shells associated with photosymbiotic activity has proven elusive. Attempts to find offsets in shell stable carbon isotope ratios (Jones et al., 1986; McConnaughey and Gillikin, 2008) were later demonstrated not to be broadly applicable between environments or species (Romanek et al., 1987; Jones and Jacobs, 1992; Killam et al., 2020). Daily oscillations in trace elemental ratios hold promise as a measure of sunlight-mediated calcification (Sano et al., 2012; de Winter et al., 2022), and recent research has quantified how trace elemental ratios vary at diurnal scales in the shells of other non-symbiotic bivalves with daily growth increments (Carré et al., 2006; Poitevin et al., 2020; de Winter et al., 2022). Trace element ratios in giant clams have been used to indicate daily and tidal cyclicity in the Miocene (Warter and Müller, 2016).

The measurement of nitrogen isotope ratios in organic matter of fossil shells could represent a new method to identify a photosymbiotic life habit in bivalves and be used to reconstruct baseline nitrogen cycling in fossil reef ecosystems. Although the variation among individuals falls within the expected values from the model, sampling multiple individuals is necessary to more accurately account for the significant variation in their respective life histories. It has been demonstrated that the nitrogen isotope composition of fossil shell-bound organic matter is resistant to diagenetic alteration in bivalve fossils (Das et al., 2021) and even in recrystallized corals of Triassic age (Tornabene et al., 2017). Future high-resolution studies investigating $\delta^{15}N$ in the shells of rudists, lithiotids, and alatochonchid bivalves in comparison to coeval bivalves of known heterotrophic life habit could help identify differences in nutrition originating from photosymbiosis. These bivalves all built reefs on top of carbonate platforms in low-latitudes during the Mesozoic that rivaled the geographic spread of modern coral reefs, yet little is known about how their natural history differed from modern photosymbiotic reef-building corals. High-resolution $\delta^{15}N$ measurements could be applied to ancient giant clams and other potentially photosymbiotic bivalves to understand how phylogeny affects the ontogeny of photosymbiosis, if the timing of its appearance during a bivalve's life is affected by nutritional stress, and to potentially reconstruct the $\delta^{15}N$ composition of DIN in reef environments of that time.

5. Conclusion

Giant clams record their diet and reliance on photosymbiosis within the nitrogen isotopes of their shell organic material. Early in life, shell $\delta^{15}N$ values for the hinge layer for three out of four shells are comparable to planktivorous Red Sea animals, but as the giant clams grow and their reliance on DIN increases, $\delta^{15}N$ values decline to be more in line with photosymbiotic soft corals from the region. The external shell layer also records the life history of the animal, displaying a less extreme ontogenetic trend due to its association with the siphonal mantle, which harbors photosymbionts from the earliest stages of the bivalve's ontogeny. One shell recorded a largely flat trend in δ15N through life, emphasizing the importance of testing multiple individuals to properly reconstruct the true breadth of pathways for development in these physiologically complex animals. The nitrogen isotopic composition of shell organic matter represents a promising system for the reconstruction of historical photosymbiosis and reef paleoenvironment, both in fossil giant clam shells and potentially as a tool to identify similar developmental signatures of photosymbiosis in extinct groups whose physiology is still poorly understood.

Data availability

Research data has been supplied via a repository: https://doi.org/10.7291/D19X13.

Declaration of Competing Interest

The authors declare that they have no known competing financial interests or personal relationships that could have appeared to influence the work reported in this paper.

Acknowledgments

The confiscated Sinai giant clam shells were obtained via a loan from the Hebrew University of Jerusalem Museum, supervised by curator Henk Mienis. The wild clam shells were obtained from the Interuniversity Institute of Eilat with a permit from the Israeli Nature & Parks Authority (#2016/41334). Funding was provided by the Zuckerman Postdoctoral Fellowship and NSF awards #1358134 and 1455258. *Tridacna* collection and processing was conducted with the assistance of Moty Ohevia, Michele Markowitz, Karen Petersen and Noam Baharav. Dana Shultz created Fig. 1. Environmental $\delta^{15}N$ sample collection and analyses were conducted with the assistance of Mark Altabet, Joe Murray, Margaret Mulholland, Scott Wankel, and the Marine Science Station, Aqaba.

Appendix A. Supplementary material

Supplementary material to this article including the clam isotope data, environmental data and code used to generate the isotopic models can be found online at https://doi.org/10.1016/j.gca.2023.08.018.

References

Agbaje, O.B.A., Wirth, R., Morales, L.F.G., Shirai, K., Kosnik, M., Watanabe, T., Jacob, D. E., 2017. Architecture of crossed-lamellar bivalve shells: the southern giant clam (Tridacna derasa, Röding, 1798). R. Soc. Open Sci. 4, 170622.

Agbaje, O.B.A., Thomas, D.E., Dominguez, J.G., Mclnerney, B.V., Kosnik, M.A., Jacob, D. E., 2019. Biomacromolecules in bivalve shells with crossed lamellar architecture. J. Mater. Sci. 54, 4952–4969.

Aharon, P., 1990. Recorders of reef environment histories: stable isotopes in corals, giant clams, and calcareous algae. Coral Reefs 10, 71–90.

Alamaru, A., Loya, Y., Brokovich, E., Yam, R., Shemesh, A., 2009. Carbon and nitrogen utilization in two species of Red Sea corals along a depth gradient: Insights from stable isotope analysis of total organic material and lipids. Geochim. Cosmochim. Acta 73, 5333–5342.

Al-Rousan, S., Al-Moghrabi, S., Pätzold, J., Wefer, G., 2003. Stable oxygen isotopes in Porites corals monitor weekly temperature variations in the northern Gulf of Aqaba, Red Sea. Coral Reefs 22, 346–356.

Badran, M.I., Rasheed, M., Manasrah, R., Al-Najjar, T., 2005. Nutrient flux fuels the summer primary productivity in the oligotrophic waters of the Gulf of Aqaba, Red Sea. Oceanologia 47.

Berman, H., Gildor, H., 2022. Phytoplankton bloom in the Gulf of Elat/Aqaba: Physical versus ecological forcing. J. Geophys. Res. Oceans 127.

Black, H.D., Andrus, C.F.T., Lambert, W.J., Rick, T.C., Gillikin, D.P., 2017. $\delta^{15}N$ values in *Crassostrea virginica* shells provides early direct evidence for nitrogen loading to Chesapeake bay. Sci. Rep. 7, 44241.

Carlos, A.A., Baillie, B.K., Kawachi, M., Maruyama, T., 1999. Phylogenetic Position of Symbiodinium (dinophyceae) Isolates from Tridacnids (bivalvia), Cardiids (bivalvia), a Sponge (porifera), a Soft Coral (anthozoa), and a Free-Living Strain. J. Phycol. 35, 1054–1062.

Carmichael, R.H., Hattenrath, T., Valiela, I., Michener, R.H., 2008. Nitrogen stable isotopes in the shell of *Mercenaria mercenaria* trace wastewater inputs from watersheds to estuarine ecosystems. Aquat. Biol. 4, 99–111.

Carré, M., Bentaleb, I., Bruguier, O., Ordinola, E., Barrett, N.T., Fontugne, M., 2006. Calcification rate influence on trace element concentrations in aragonitic bivalve shells: Evidences and mechanisms. Geochim. Cosmochim. Acta 70, 4906–4920.

Chambers, C.N., 2007. Pasua (Tridacna maxima) size and abundance in Tongareva Lagoon, Cook Islands. SPC Trochus Info. Bull. 13, 7–12.

Chan, K.R., Todd, P.A., Chou, L.M., 2008. An allometric analysis of juvenile fluted giant clam shells (*Tridacna squamosa* L.). J. Conchol. 39, 621.

Chen, Y., Mills, S., Street, J., Golan, D., Post, A., Jacobson, M., Paytan, A., 2007. Estimates of atmospheric dry deposition and associated input of nutrients to Gulf of Aqaba seawater. J. Geophys. Res, Atmospheres, p. 112.

Coplen, T.B., Brand, W.A., Gehre, M., Gröning, M., Meijer, H.A.J., Toman, B., Verkouteren, R.M., 2006. New Guidelines for $\delta^{13}C$ Measurements. Anal. Chem. 78, 2439–2441.

Darrow, E.S., Carmichael, R.H., Andrus, C.F.T., Jackson, H.E., 2017. From middens to modern estuaries, oyster shells sequester source-specific nitrogen. Geochim. Cosmochim. Acta 202, 39–56.

Das, S., Judd, E.J., Uveges, B.T., Ivany, L.C., Junium, C.K., 2021. Variation in $\delta^{15}N$ from shell-associated organic matter in bivalves: Implications for studies of modern and fossil ecosystems. Palaeogeogr. Palaeoclimatol. Palaeoecol. 562, 110076.

de Winter, N.J., Goderis, S., Malderen, S.J.M.V., Sinnesael, M., Vansteenberge, S., Snoeck, C., Belza, J., Vanhaecke, F., Claeys, P., 2020. Subdaily-Scale Chemical Variability in a *Torreites sanchezi* Rudist Shell: Implications for Rudist Paleobiology and the Cretaceous Day-Night Cycle. Paleoceanogr. Paleoclimatology 35.

de Winter, N.J., Killam, D., Fröhlich, L., de Nooijer, L., Boer, W., Schöne, B.R., Thébault, J., Reichart, G.-J., 2022. Ultradian rhythms in shell composition of photosymbiotic and non-photosymbiotic mollusks. EGUsphere 1–61.

Dreier, A., Loh, W., Blumenberg, M., Thiel, V., Hause-Reitner, D., Hoppert, M., 2014. The isotopic biosignatures of photo-vs. thiotrophic bivalves: are they preserved in fossil shells? Geobiology 12, 406–423.

Elfwing, T., Blidberg, E., Sison, M., Tedengren, M., 2003. A comparison between sites of growth, physiological performance and stress responses in transplanted *Tridacna gigas*. Aquaculture 219, 815–828.

Erler, D.V., Farid, H.T., Glaze, T.D., Carlson-Perret, N.L., Lough, J.M., 2020. Coral skeletons reveal the history of nitrogen cycling in the coastal Great Barrier Reef. Nat. Commun. 11, 1–8.

Fitt, W.K., Rees, T.A.V., Braley, R.D., Lucas, J.S., Yellowlees, D., 1993. Nitrogen flux in giant clams: size-dependency and relationship to zooxanthellae density and clam biomass in the uptake of dissolved inorganic nitrogen. Mar. Biol. 117, 381–386.

Foster, R.A., Paytan, A., Zehr, J.P., 2009. Seasonality of N2 fixation and nifH gene diversity in the Gulf of Aqaba (Red Sea). Limnol. Oceanogr. 54, 219–233.

Frankowiak, K., Wang, X.T., Sigman, D.M., Gothmann, A.M., Kitahara, M.V., Mazur, M., Meibom, A., Stolarski, J., 2016. Photosymbiosis and the expansion of shallow-water corals. Sci. Adv. 2, e1601122.

Fraser, N.M., Bottjer, D.J., Fischer, A.G., 2004. Dissecting "Lithiotis" Bivalves: Implications for the Early Jurassic Reef Eclipse. PALAIOS 19, 51–67.

Fujii, T., Tanaka, Y., Maki, K., Saotome, N., Morimoto, N., Watanabe, A., Miyajima, T., 2020. Organic Carbon and Nitrogen Isoscapes of Reef Corals and Algal Symbionts: Relative Influences of Environmental Gradients and Heterotrophy. Microorganisms 8, 1221.

Gannon, M.E., Pérez-Huerta, A., Aharon, P., Street, S.C., 2017. A biomineralization study of the Indo-Pacific giant clam *Tridacna gigas*. Coral Reefs 36, 503–517.

Gillikin, D.P., Lorrain, A., Jolivet, A., Kelemen, Z., Chauvaud, L., Bouillon, S., 2017. High-resolution nitrogen stable isotope sclerochronology of bivalve shell carbonate-bound organics. Geochim. Cosmochim. Acta 200, 55–66.

Gnaiger, E., Bitterlich, G., 1984. Proximate biochemical composition and caloric content calculated from elemental CHN analysis: a stoichiometric concept. Oecologia 62, 289–298.

Graniero, L.E., Grossman, E.L., O'Dea, A., 2016. Stable isotopes in bivalves as indicators of nutrient source in coastal waters in the Bocas del Toro Archipelago. Panama. *PeerJ* 4, e2278.

Hardy, J.T., Hardy, S.A., 1969. Ecology of Tridacna in Palau. Pac. Sci. 23, 467–472.

Hawkins, A.J.S., Klumpp, D.W., 1995. Nutrition of the giant clam Tridacna gigas (L.). II. Relative contributions of filter-feeding and the ammonium-nitrogen acquired and recycled by symbiotic alga towards total nitrogen requirements for tissue growth and metabolism. J. Exp. Mar. Biol. Ecol. 190, 263–290.

Heikoop, J., Dunn, J., Risk, M., Tomascik, T., Schwarcz, H., Sandeman, I., Sammarco, P., 2000. $\delta^{15}N$ and $\delta^{13}C$ of coral tissue show significant inter-reef variation. Coral Reefs-J. Int. Soc. Reef Stud. 19, 189–193.

Helber, S.B., Winters, G., Stuhr, M., Belshe, E.F., Bröhl, S., Schmid, M., Reuter, H., Teichberg, M., 2021. Nutrient History Affects the Response and Resilience of the Tropical Seagrass *Halophila stipulacea* to Further Enrichment in Its Native Habitat. Front. Plant Sci. 12.

Ip, Y.K., Hiong, K.C., Goh, E.J.K., Boo, M.V., Choo, C.Y.L., Ching, B., Wong, W.P., Chew, S.F., 2017. The whitish inner mantle of the giant clam, *Tridacna squamosa*, expresses an apical Plasma Membrane Ca^{2+}-ATPase (PMCA) which displays light-dependent gene and protein expressions. Front. Physiol. 8.

Ip, Y.K., Hiong, K.C., Teng, J.H.Q., Boo, M.V., Choo, C.Y.L., Wong, W.P., Chew, S.F., 2020. The fluted giant clam (*Tridacna squamosa*) increases nitrate absorption and upregulates the expression of a homolog of SIALIN (H+:2NO3− cotransporter) in the ctenidium during light exposure. Coral Reefs 39, 451–465.

Jones, D.S., Jacobs, D.K., 1992. Photosymbiosis in *Clinocardium nuttalli*: Implications for tests of photosymbiosis in fossil molluscs. PALAIOS 7, 86–95.

Jones, D.S., Williams, D.F., Romanek, C.S., 1986. Life history of symbiont-bearing giant clams from stable isotope profiles. Science 231, 46–48.

Killam, D., 2018. The When, How and Why of Bivalve Shell Growth: Sclerochronology as a Tool to Understand Physiology in Jurassic and Future Oceans. UC Santa Cruz.

Killam, D., Al-Najjar, T., Clapham, M., 2021. Giant clam growth in the Gulf of Aqaba is accelerated compared to fossil populations. Proc. R. Soc. B Biol. Sci. 288, 20210991.

Killam, D.E., Clapham, M.E., 2018. Identifying the ticks of bivalve shell clocks: Seasonal growth in relation to temperature and food supply. PALAIOS 33, 228–236.

Killam, D., Thomas, R., Al-Najjar, T., Clapham, M., 2020. Interspecific and intrashell stable isotope variation among the Red Sea Giant Clams. Geochem. Geophys. Geosyst. 21.

Klumpp, D.W., Bayne, B.L., Hawkins, A.J.S., 1992. Nutrition of the giant clam *Tridacna gigas* (L.) I. Contribution of filter feeding and photosynthates to respiration and growth. J. Exp. Mar. Biol. Ecol. 155, 105–122.

Kürten, B., Al-Aidaroos, A.M., Struck, U., Khomayis, H.S., Gharbawi, W.Y., Sommer, U., 2014. Influence of environmental gradients on C and N stable isotope ratios in coral reef biota of the Red Sea, Saudi Arabia. *J. Sea Res.* 85, 379–394.

Labiosa, R.G., Arrigo, K.R., Genin, A., Monismith, S.G., van Dijken, G., 2003. The interplay between upwelling and deep convective mixing in determining the seasonal phytoplankton dynamics in the Gulf of Aqaba: Evidence from SeaWiFS and MODIS. Limnol. Oceanogr. 48, 2355–2368.

Lachapelle, E., 2020. Comprehensive culture methods of giant clams (*Tridacna* spp.): Simplicity is key. Curr. Top. Moll. Aquac. 9.

Li, J., Volsteadt, M., Kirkendale, L., Cavanaugh, C., 2018. Characterizing photosymbiosis between *Fraginae bivalves* and Symbiodinium using phylogenetics and stable isotopes. Front. Ecol. Evol. 6, 45.

Lipps, J.H., Stanley, G.D., 2016. Photosymbiosis in past and present reefs. In: Coral Reefs at the Crossroads Coral Reefs of the World. Springer, Dordrecht, pp. 47–68.

Lojen, S., Spanier, E., Tsemel, A., Katz, T., Eden, N., Angel, D.L., 2005. $\delta^{15}N$ as a natural tracer of particulate nitrogen effluents released from marine aquaculture. Mar. Biol. 148, 87–96.

Loya, Y., 2004. The coral reefs of Eilat — Past, present and future: three decades of coral community structure studies. In: Rosenberg, E., Loya, Y. (Eds.), Coral Health and Disease. Springer Berlin Heidelberg, Berlin, Heidelberg, pp. 1–34.

Lucas, J.S., 1994. The biology, exploitation, and mariculture of giant clams (Tridacnidae). Rev. Fish. Sci. 2, 181–223.

Lucas, J.S., Nash, W.J., Crawford, C.M., Braley, R.D., 1989. Environmental influences on growth and survival during the ocean-nursery rearing of giant clams, Tridacna gigas (L.). Aquaculture 80, 45–61.

Mahmoud, M.A.M., Zamzamy, R.M., Dar, M.A., Mohammed, T.A.A., 2018. Biochemical assessment in the edible parts of *Tridacna maxima* Röding, 1798 collected from the Egyptian Red Sea, Egypt. J. Aquat. Res. 44, 257–262.

McClelland, J.W., Holl, C.M., Montoya, J.P., 2003. Relating low $\delta^{15}N$ values of zooplankton to N_2-fixation in the tropical North Atlantic: insights provided by stable isotope ratios of amino acids. Deep Sea Res. Pt. I: Oceanogr. Res. Pap. 50, 849–861.

McConnaughey, T.A., Gillikin, D.P., 2008. Carbon isotopes in mollusk shell carbonates. Geo-Mar. Lett. 28, 287–299.

Möbius, J., 2013. Isotope fractionation during nitrogen remineralization (ammonification): Implications for nitrogen isotope biogeochemistry. Geochim. Cosmochim. Acta 105, 422–432.

Mohammed, T.A.A., Mohamed, M.H., Zamzamy, R.M., Mahmoud, M.A.M., 2019. Growth rates of the giant clam Tridacna maxima (Röding, 1798) reared in cages in the Egyptian Red Sea, Egypt. J. Aquat. Res.

Munro, J.L., 1982. Estimation of the parameters of the von Bertalanffy growth equation from recapture data at variable time intervals. ICES J. Mar. Sci. 40, 199–200.

Murray, J., Prouty, N.G., Peek, S., Paytan, A., 2019. Coral skeleton $\delta^{15}N$ as a tracer of historic nutrient loading to a coral reef in Maui, Hawaii. Sci. Rep. 9, 5579.

Neo, M.L., Wabnitz, C.C., Braley, R.D., Heslinga, G.A., Fauvelot, C., Van Wynsberge, S., Andréfouët, S., Waters, C., Tan, A.-S.-H., 2017. Giant clams (Bivalvia: Cardiidae: Tridacninae): a comprehensive update of species and their distribution, current threats and conservation status. Oceanogr. Mar. Biol. Annu. Rev. 55, 87–387.

Pätzold, J., Heinrichs, J.P., Wolschendorf, K., Wefer, G., 1991. Correlation of stable oxygen isotope temperature record with light attenuation profiles in reef-dwelling *Tridacna* shells. Coral Reefs 10, 65–69.

Peharda, M., Gillikin, D.P., Schöne, B.R., Verheyden, A., Uvanović, H., Markulin, K., Šarić, T., Janeković, I., Župan, I., 2022. Nitrogen isotope schlerochronology – Insights into coastal environmental conditions and *Pinna nobilis* ecology. Front. Mar. Sci. 8, 816879.

Pitcher, T.J., Macdonald, P.D.M., 1973. Two models for seasonal growth in fishes. J. Appl. Ecol. 10, 599–606.

Poitevin, P., Chauvaud, L., Pécheyran, C., Lazure, P., Jolivet, A., Thébault, J., 2020. Does trace element composition of bivalve shells record ultra-high frequency environmental variations? Mar. Environ. Res. 158, 104943.

Polissar, P.J., Fulton, J.M., Junium, C.K., Turich, C.C., Freeman, K.H., 2009. Measurement of ^{13}C and ^{15}N isotopic composition on nanomolar quantities of C and N. Anal. Chem. 81, 755–763.

Posenato, R., Bassi, D., Nebelsick, J.H., 2013. *Opisoma excavatum* Boehm, a Lower Jurassic photosymbiotic alatoform-chambered bivalve. Lethaia 46, 424–437.

R Core Team, 2013. R: A Language and Environment for Statistical Computing.

Rasheed, M., Badran, M.I., Richter, C., Huettel, M., 2002. Effect of reef framework and bottom sediment on nutrient enrichment in a coral reef of the Gulf of Aqaba, Red Sea. Mar. Ecol. Prog. Ser. 239, 277–285.

Ren, H., Chen, Y.-C., Wang, X.T., Wong, G.T.F., Cohen, A.L., DeCarlo, T.M., Weigand, M. A., Mii, H.-S., Sigman, D.M., 2017. 21st-century rise in anthropogenic nitrogen deposition on a remote coral reef. Science 356, 749–752.

Richter, C., Roa-Quiaoit, H., Jantzen, C., Al-Zibdah, M., Kochzius, M., 2008. Collapse of a new living species of giant clam in the Red Sea. Curr. Biol. CB 18, 1349–1354.

Roa-Quiaoit, H.A.F., 2005. The ecology and culture of giant clams (Tridacnidae) in the Jordanian sector of the Gulf of Aqaba, Red Sea. PhD Univ. Brem.

Romanek, C., Jones, D., Williams, D., Krantz, D., 1987. Stable isotopic investigation of physiological and environmental changes recorded in shell carbonate from the giant clam *Tridacna maxima*.

Rossbach, S., Cardenas, A., Perna, G., Duarte, C.M., Voolstra, C.R., 2019. Tissue-specific microbiomes of the Red Sea Giant clam *Tridacna maxima* highlight differential abundance of Endozoicomonadaceae. Front. Microbiol. 10.

Sano, Y., Kobayashi, S., Shirai, K., Takahata, N., Matsumoto, K., Watanabe, T., Sowa, K., Iwai, K., 2012. Past daily light cycle recorded in the strontium/calcium ratios of giant clam shells. Nat. Commun. 3, ncomms1763.

Schöne, B.R., Huang, Q., 2021. Ontogenetic $\delta^{15}N$ trends and multidecadal variability in shells of the bivalve mollusc, *Arctica islandica*. Front. Mar. Sci. 8, 748593.

Schöne, B.R., Surge, D.M., 2012. Part N, Revised, Volume 1, Chapter 14: bivalve sclerochronology and geochemistry. Treatise Online 46, 1–24.

Schwartzmann, C., Durrieu, G., Sow, M., Ciret, P., Lazareth, C.E., Massabuau, J.-C., 2011. In situ giant clam growth rate behavior in relation to temperature: A one-year coupled study of high-frequency noninvasive valvometry and sclerochronology. Limnol. Oceanogr. 56, 1940–1951.

Shellenbarger, G.G., Monismith, S.G., Genin, A., Paytan, A., 2006. The importance of submarine groundwater discharge to the near shore nutrient supply in the Gulf of Aqaba (Israel). Limnol. Oceanogr. 51, 1876–1886.

Taylor, J.D., Layman, M., 1972. The mechanical properties of bivalve (Mollusca) shell structures. Palaeontology 15, 73–87.

Teh, L.S.X., Poo, J.S.T., Boo, M.V., Chew, S.F., Ip, Y.K., 2021. Using glutamine synthetase 1 to evaluate the symbionts' potential of ammonia assimilation and their responses to illumination in five organs of the giant clam, *Tridacna squamosa*. Comp. Biochem. Physiol. A Mol. Integr. Physiol. 255, 110914.

Tornabene, C., Martindale, R.C., Wang, X.T., Schaller, M.F., 2017. Detecting photosymbiosis in *Fossil scleractinian* corals. Sci. Rep. 7, 9465.

Vermeij, G.J., 2013. The evolution of molluscan photosymbioses: A critical appraisal. Biol. J. Linn. Soc. 109, 497–511.

Vicentuan-Cabaitan, K., Neo, M.L., Eckman, W., Teo, S.L., Todd, P.A., 2014. Giant clam shells host a multitude of epibionts. Bull. Mar. Sci. 90, 795–796.

Vokhshoori, N.L., Tipple, B.J., Teague, L., Bailess, A., McCarthy, M.D., 2022. Calibrating bulk and amino acid $\delta^{13}C$ and $\delta^{15}N$ isotope ratios between bivalve soft tissue and shell for paleoecological reconstructions. Palaeogeogr. Palaeoclimatol. Palaeoecol. 595, 110979.

Wankel, S.D., Chen, Y., Kendall, C., Post, A.F., Paytan, A., 2010. Sources of aerosol nitrate to the Gulf of Aqaba: Evidence from $\delta^{15}N$ and $\delta^{18}O$ of nitrate and trace metal chemistry. Mar. Chem. 120, 90–99.

Warter, V., Müller, W., 2016. Daily growth and tidal rhythms in Miocene and modern giant clams revealed via ultra-high resolution LA-ICPMS analysis—A novel methodological approach towards improved sclerochemistry. Palaeogeogr. Palaeoclimatol. Palaeoecol.

Whitney, N.M., Johnson, B.J., Dostie, P.T., Luzier, K., Wanamaker, A.D., 2019. Paired bulk organic and individual amino acid $\delta^{15}N$ analyses of bivalve shell periostracum: A paleoceanographic proxy for water source variability and nitrogen cycling processes. Geochim. Cosmochim. Acta 254, 67–85.

Wisshak, M., Neumann, C., 2018. Large dendrinids meet giant clam: the bioerosion trace fossil *Neodendrina carnelia* igen. et isp. n. in a Tridacna shell from Pleistocene-Holocene coral reef deposits, Red Sea, Egypt. Foss. Rec. 21, 1–9.

Yancey, T.E., Stanley, G.D., 1999. Giant alatoform bivalves in the Upper Triassic of western North America. Palaeontology 42, 1–23.

Yau, A.-J.-Y., Fan, T.-Y., 2012. Size-dependent photosynthetic performance in the giant clam *Tridacna maxima*, a mixotrophic marine bivalve. Mar. Biol. 159, 65–75.